

Hydrocarbyl Ligand “Tuning” of the Pt^{II/IV} Redox Potential

Andrei N. Vedernikov,* Maren Pink, and Kenneth G. Caulton*

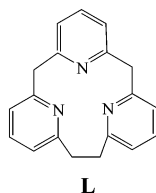
Department of Chemistry, Indiana University, Bloomington, Indiana 47405

Received June 26, 2003

The potentially tridentate macrocycle [2.1.1]-(2,6)-pyridinophane (L) enables the transient LPt^{II}(CH₃)⁺ to cleave the C–H bond of two molecules of C₆F₅H. The resulting product has two aryl groups on Pt but, in contrast to nonfluorinated analogue, varies in its location of the cleaved H, as is evident from the two products (HL⁺)Pt^{II}R₂ and (η³-L)-Pt^{IV}H(R)₂⁺. At equilibrium, the related example where R = CH₃ is purely the Pt^{IV} redox isomer, which with R = C₆H₅ shows detectable populations of both isomers, and with R = C₆F₅ is purely the pyridine-protonated (HL⁺)Pt^{II} redox isomer. All species show a hydrogen bond from the pyridinium proton to Pt^{II}. Consistent with the idea that electron-withdrawing R makes platinum(II) more resistant to oxidation (i.e., a proton on Pt), and thus less Brønsted basic, the ¹J_{PtH} coupling constant falls in the series R = Me (90 Hz), R = C₆H₅ (86 Hz), and R = C₆F₅ (63 Hz).

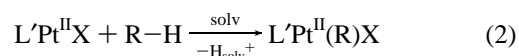
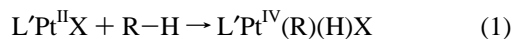
Introduction

Transition-metal basicity, nucleophilicity, and reducing power are often strongly correlated parameters which can therefore influence a broad range of chemical reactivity. We have reported earlier that a CH₂Cl₂-solvated transient LPt(CH₃)⁺, involving the preorganized-geometry macrocyclic ligand L,¹ has the ability to cleave a wide range of C–H bonds, including alkanes.^{2,3}

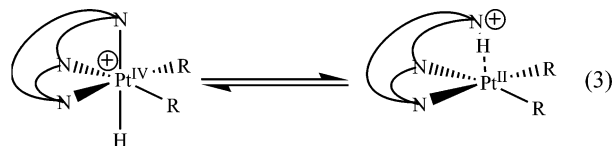


Two limiting cases of mechanistic extremes are considered for alkane (R–H) activation with Pt^{II}.^{4,5} Oxidative addition, eq 1, involving a change of metal oxidation state is an alternative to the nonredox electrophilic substitution of

hydrogen (eq 2), which requires a base to remove H⁺ from R–H σ-bonded to Pt^{II}.



One of these mechanisms, eq 1, is also known in platinum(II)/arene chemistry.^{6,7} In principle, either *product* might be obtained in a single system because it has been shown that the two different products in eqs 1 and 2 can coexist in equilibrium, eq 3 (R = Ph).² Thus, in (η²-L)-



PtR⁺, the pendant pyridine of η²-L can participate either by binding to the emerging Pt^{IV} center during C–H oxidative addition or by binding H⁺ during electrophilic hydrogen substitution. With (η²-L)PtR⁺ with R = Ph as a reference, we can expect that small changes of electronic or steric

* Authors to whom correspondence should be addressed. E-mail: caulton@indiana.edu (K.G.C.).

(1) Vedernikov, A. N.; Pink, M.; Caulton, K. G. *J. Org. Chem.* **2003**, *68*, 4806.

(2) Vedernikov, A. N.; Huffman, J. C.; Caulton, K. G. *Chem. Commun.* **2003**, 358.

(3) Vedernikov, A. N.; Huffman, J. C.; Caulton, K. G. *New J. Chem.* **2003**, *27*, 665.

(4) Wick, D. D.; Goldberg, K. I. *J. Am. Chem. Soc.* **1997**, *119*, 10235.

(5) Siegbahn, P. E. M.; Crabtree, R. H. *J. Am. Chem. Soc.* **1996**, *118*, 4442.

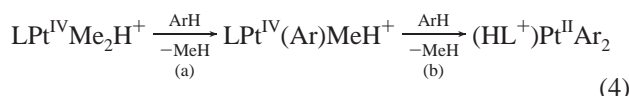
(6) (a) Reinartz, S.; White, P. S.; Brookhart, M.; Templeton, J. L. *Organometallics* **2001**, *20*, 1709. (b) Norris, C. M.; Reinartz, S.; White, P. S.; Templeton, J. L. *Organometallics* **2002**, *21*, 5649.

(7) (a) Zhong, H. A.; Labinger, J. A.; Bercaw, J. E. *J. Am. Chem. Soc.* **2002**, *124*, 1378. (b) Johansson, L.; Tilset, M.; Labinger, J. A.; Bercaw, J. E. *J. Am. Chem. Soc.* **2000**, *122*, 10846. (c) Peters, R. G.; White, S.; Roddick, D. M. *Organometallics* **1998**, *17*, 4493.

effects in the complex can affect the product distribution in equilibrium 3. Here we demonstrate a concrete example of this effect. Concurrently, we show how the basicity of Pt^{II} in the corresponding product of electrophilic hydrogen substitution, (HL⁺)Pt^{II}R₂, is reflected in the observed value of the Pt⋯HN⁺ coupling constant.

Results

Electrophilic Hydrogen Substitution in C₆F₅H. Pentafluorobenzene (50:1 mole ratio) reacted with a CD₂Cl₂ solution of LPtMe₂H⁺ (BAR^F₄ salt) at 22 °C in the course of 24 h to produce cleanly the N-protonated bis(pentafluorophenyl)platinum(II) complex, eq 4 (Ar = C₆F₅). Methane (¹H



NMR evidence) evolution was accompanied by the complete disappearance of the high-field ¹H NMR hydride signal of LPtMe₂H⁺ at −21.65 ppm. Growth of a low-field signal (+16.3 ppm), very broad at 22 °C and more narrow at −40 °C, was evidence of the NH⁺ proton, with satellites due to Pt–H coupling of 63 Hz. The latter chemical shift and coupling are diagnostic of hydrogen bonding to the metal,^{8–11} which is evidence of the basicity of square-planar Pt^{II} via the doubly occupied d_{z²} orbital. Heating the reaction mixture for 96 h at 80 °C did not affect its composition; no high-field Pt–H resonances and thus no traces of hydridoplatinum complexes were detected, consistent with (HL⁺)Pt^{II}Ar₂ being the thermodynamic product in the case of Ar = C₆F₅. In contrast to the phenyl analogue,² no intermediate LPt(Ar)MeH⁺ (Ar = C₆F₅ vs Ph, eq 4) was observed by NMR spectroscopy. Its lower stability is presumably due to the stronger electron-withdrawing character and bulkiness of C₆F₅ versus Ph. The ¹⁹F NMR spectrum shows four broad signals due to the *m*- and *o*-fluorines, indicating slowed rotation about Pt–aryl bonds at 22 °C along with two sharp triplets of *p*-fluorines of two nonequivalent pentafluorophenyl ligands. At −40 °C the rotation becomes very slow on the NMR time scale, so that signals of *m*- and *o*-fluorines appear as eight sharp multiplets.

X-ray Diffraction Structure Determination of the BAR^F₄ Salt of (HL⁺)Pt(C₆F₅)₂. Slow evaporation of a CH₂Cl₂–pentane solution of [(HL⁺)Pt(C₆F₅)₂]BAR^F₄ yields small crystals suitable for X-ray diffraction structure determination (Figure 1 and Tables 1 and 2) using long frame times and a SMART 6000 system.

The coordination geometry around Pt is faithful to *cis*-disubstituted planar; *cis* angles around Pt sum to 358.8°. The species lacks mirror symmetry because the pendant pyri-

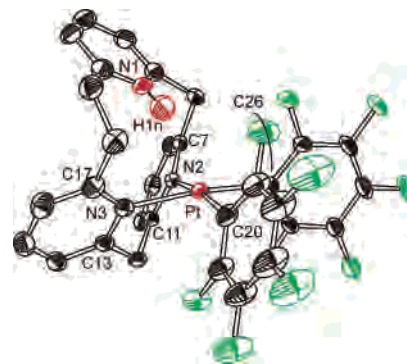


Figure 1. ORTEP drawing of the non-hydrogen atoms of (LH⁺)Pt(C₆F₅)₂, showing selected atom labeling and the hydrogen bonding of the pyridinium acidic proton to Pt.

Table 1. Crystal Data and Structure Refinement for [(LH⁺)Pt(C₆F₅)₂](BAR^F₄) in CH₂Cl₂

empirical formula	C ₆₃ H ₃₀ BF ₃₄ N ₃ Pt	
fw	1680.80	
cryst color, shape, size	colorless block, 0.20 × 0.15 × 0.13 mm ³	
temp	137(2) K	
wavelength	0.71073 Å	
cryst syst, space group	monoclinic, P2(1)/c	
unit cell dimens	<i>a</i> = 18.9201(19) Å <i>b</i> = 13.3663(12) Å <i>c</i> = 28.588(4) Å	$\alpha = 90^\circ$ $\beta = 95.691(7)^\circ$ $\gamma = 90^\circ$
vol	7194.0(15) Å ³	
Z	4	
density(calcd)	1.552 Mg/mm ³	
abs coeff	2.077 mm ^{−1}	
<i>F</i> (000)	3272	
no. of independent reflns	21015 [<i>R</i> (int) = 0.0529]	
no. of data/restraints/params	21015/24/948	
GOF on <i>F</i> ²	1.065 ^a	
final <i>R</i> indices [<i>I</i> > 2σ(<i>I</i>)]	<i>R</i> 1 = 0.0375 ^b	w <i>R</i> 2 = 0.0909 ^c
<i>R</i> indices (all data)	<i>R</i> 1 = 0.0476 ^b	w <i>R</i> 2 = 0.0949 ^c
largest diff peak and hole	3.387 and −1.594 e [−] Å ^{−3}	

^a GOF = [Σ[w(*F*_o² − *F*_c²)]/(*N*_{observns} − *N*_{params})]^{1/2}, all data. ^b *R*1 = Σ(|*F*_o − *F*_c|)/Σ|*F*_o|. ^c w*R*2 = [Σ[w(*F*_o² − *F*_c²)]/Σ[w(*F*_o²)]]^{1/2}.

Table 2. Selected Bond Lengths (Å) and Angles (deg) for the Cation (LH⁺)Pt(C₆F₅)₂

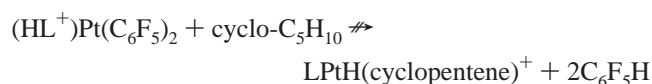
Pt1	C26		2.016(3)
Pt1	C20		2.020(3)
Pt1	N3		2.091(2)
Pt1	N2		2.100(2)
Pt1	H1n		2.428
C26	Pt1	C20	87.98(13)
C26	Pt1	N3	172.01(10)
C20	Pt1	N3	93.49(12)
C26	Pt1	N2	92.96(10)
C20	Pt1	N2	170.71(11)
N3	Pt1	N2	84.35(9)
C11	N2	Pt1	112.91(17)
C7	N2	Pt1	128.02(18)
C17	N3	Pt1	126.9(2)
C13	N3	Pt1	113.78(19)
N1	H1n	Pt1	167.52

dinium moiety is tethered by one CH₂ and one (CH₂)₂ link. Because of the single CH₂ link between N2 and N3, the N2–Pt–N3 angle is small (84.35(9)°). Macrocyclic ring constraints also cause ~8° misalignment of the N2 and N3 pyridine lone pairs from an ideal ∠Pt–N–C(*ortho*) of 120°. The pyridinium ring orients the N–H proton toward (not away from) Pt, with a H⁺–Pt distance, 2.428 Å, which is

- (8) Puddephatt, R. J. *Coord. Chem. Rev.* **2001**, 219–221, 157.
 (9) Casas, J. M.; Falvello, L. R.; Fornies, J.; Martin, A.; Welch, A. J. *Inorg. Chem.* **1996**, 35, 6009.
 (10) (a) Cauty, A. J.; van Koten, G. *Acc. Chem. Res.* **1995**, 28, 406. (b) Hambley, T. W. *Inorg. Chem.* **1998**, 37, 3767.
 (11) (a) Yao, W.; Eisenstein, O.; Crabtree, R. H. *Inorg. Chim. Acta* **1997**, 254, 105. (b) Braga, D.; Grepioni, F.; Tedesco, E.; Biradha, K.; Desiraju, G. R. *Organometallics* **1997**, 16, 1846.

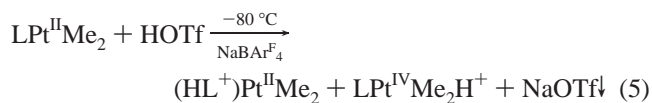
among the shortest observed^{9,11} for such hydrogen bonding to planar Pt^{II}. The angle Pt–H1n–N1 is 167.52° as is common for hydrogen-bonded platinum(II) compounds.^{9–11} There are no short contacts of this proton with C₆F₅ fluorines.

Attempted Use of (HL⁺)Pt^{II}(C₆F₅)₂ for Conversion of Alkane. The equilibrium pair in eq 3 (R = Ph) has shown the ability to react with ethane and cyclopentane to give the corresponding LPtH(olefin)⁺ and benzene.² This is because LPtPh₂H⁺ is able to slowly eliminate benzene at 22 °C and the resulting transient LPtPh⁺ adds ethane, then loses benzene, and eliminates β-H. The contrasting *reluctance* of (HL⁺)Pt(C₆F₅)₂ to eliminate C₆F₅H is shown by the fact that, when heated with 25 vol % cyclopentane in a sealed NMR tube at 80 °C for 24 h, it shows no change in its ¹H NMR spectrum. Thus, no LPtH(olefin)⁺ complex forms.



This is consistent with the preferential strengthening of the M–C₆X₅ vs X₅C₆–H bond¹² when X = F, which strongly disfavors ArH elimination from LPtAr₂H⁺ in the case of Ar = C₆F₅ as compared with Ar = C₆H₅.

Formation and Isomerization of (HL⁺)Pt^{II}Me₂. This molecule is both thermodynamically and kinetically unstable even at –50 °C. Protonation of LPt^{II}Me₂ with triflic acid in CH₂Cl₂ in the presence of NaBAR₄^F at –80 °C (eq 5)¹³ forms



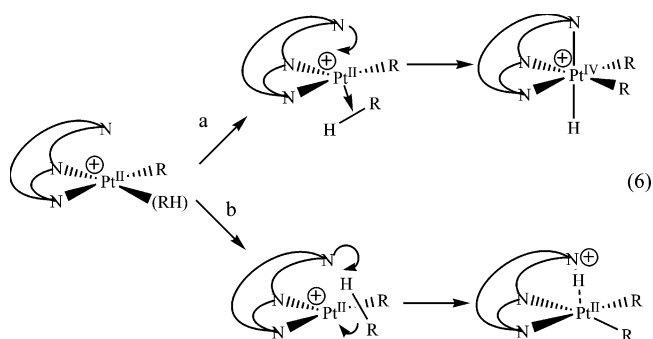
(HL⁺)PtMe₂ in 8% yield along with two isomeric LPt^{IV}Me₂H⁺ complexes, symmetrical (4%) and unsymmetrical (88%). The ¹H NMR data reveal the former to have the unsymmetrical binding of the pyridinophane to Pt, as is true of the reagent LPtMe₂,¹⁴ and the observed ¹H NMR signal at +17.17 ppm is consistent with concerted protonation directly at the pendant pyridine. This species shows a NH⋯Pt coupling constant of 90 Hz, this being larger than that of either the C₆H₅ (86 Hz) or C₆F₅ (63 Hz) analogue.

Raising the temperature to –45 °C causes rapid (τ_{1/2} = 8 min) isomerization of (HL⁺)PtMe₂ into the thermodynamically *more stable* product *sym*-LPt^{IV}Me₂H⁺.³ Thus, the equilibrium in eq 3 lies to the left side for R = Me.

Discussion

CH Bond Activation with LPtR⁺: Oxidative Addition versus Electrophilic Substitution. Analyzing the second step in eq 4, we can consider two orientations of a sub-

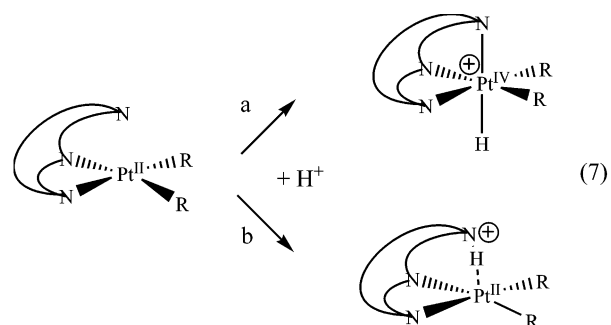
strate R–H bond to a Pt^{II} center in a complex of RH¹⁵ in the proposed reactive transient (η²-L)PtR(R–H)⁺,^{2,3} eqs 6a and 6b.



In eq 6a, the pendant nitrogen can lower the activation energy by incipient formation of the third Pt–N bond. In eq 6b, the H–R bond orientation permits CH bond cleavage *assisted* by the pendant nitrogen. The latter product is then stabilized by an intramolecular metal–hydrogen bond, Pt⋯•HN⁺, to the platinum d_{z²} orbital.¹⁰

Considering eq 6b (R = C₆F₅) from the point of view of synthetic utility, we believe it represents the *first* example of the synthesis of pentafluorophenylplatinum(II) complexes by *direct metalation* of the corresponding *fluorohydrocarbon*.¹⁶

Consider now formation of (HL⁺)Pt^{II}R₂ and LPt^{IV}R₂H⁺ isomers by a different method: protonation of species LPt^{II}R₂ with R = C₆F₅, Ph, and Me, eq 7.^{2,3} All of these LPt^{II}R₂



species are characterized by virtually the same basicity of the pendant nitrogen but by different basicities of the metal atom bearing different ligands R. The steric size of R may also influence the site of protonation. For example, ¹H NMR data show that rotation about the Pt–Ar bond in (HL⁺)Pt^{II}Ar₂ at 22 °C is fast for Ar = Ph, but slowed for Ar = C₆F₅, thus indicating larger steric bulk and/or Pt–aryl π bonding in the latter case.

Addition of a proton to the more electron-rich platinum atom in LPt^{II}Me₂ leads ultimately to the formation of the

(12) Clot, E.; Besora, M.; Maseras, F.; Megret, C.; Eisenstein, O.; Oelckers, B.; Perutz, R. N. *Chem. Commun.* **2003**, 490.

(13) Triflate coordinates to the Pt^{II} transient, quenching the C–H cleavage chemistry. The sodium in NaBAR₄^F precipitates NaOTf, and (BAR₄^F) leaves the transient highly unsaturated.

(14) Vedernikov, A. N.; Huffmann, J. C.; Caulton, K. G. *Inorg. Chem.* **2003**, *41*, 6867.

(15) (a) Jones, W. D. *Acc. Chem. Res.* **2003**, *36*, 140. (b) Flood, T. C.; Janak, K. E.; Imura, M.; Zhen, H. *J. Am. Chem. Soc.* **2000**, *122*, 6783. (c) Childs, G. I.; Colley, C. S.; Dyer, J.; Grills, D. C.; Sun, X.-Z.; Yang, J.; George, M. W. *J. Chem. Soc., Dalton Trans.* **2000**, 1901. (d) Hall, C.; Perutz, R. N. *Chem. Rev.* **1996**, *96*, 3125. (e) Bengali, A. A.; Arndtsen, B. A.; Burger, P. M.; Schultz, R. H.; Weiller, B. H.; Kyle, K. R.; Moore, C. B.; Bergman, R. G. *Pure Appl. Chem.* **1995**, *67*, 281.

(16) Clot, E.; Oelckers, B.; Klahn, A. H.; Eisenstein, O.; Perutz, R. N. *J. Chem. Soc., Dalton Trans.* **2003**, 4065.

most stable, platinum(IV) isomer, *sym*-LPt^{IV}R₂H⁺,³ eq 7a, while in the case of the electron-poor platinum center in LPt^{II}(C₆F₅)₂ the most stable product of its protonation should be the (HL⁺)Pt^{II}R₂ species, eq 7b. In the case of R = Ph, platinum(II) and platinum(IV) redox isomers are formed, by protonation at low temperature, in a 9:1 thermodynamic ratio.² Thus, increasing the electron-withdrawing character and steric bulk of R thermodynamically favors the product of reaction 6b (7b) over that of reaction 6a (7a).

Pt^{II}–HX Hydrogen Bonding in L''Pt^{II}R₂ Complexes. Another measure of the relative basicity of the Pt^{II} center in LPt^{II}R₂ species, besides the value of the equilibrium constant of eq 3, might be the magnitude of the Pt–H coupling constant in (HL⁺)Pt^{II}R₂. This decreases according to R = Me > Ph > C₆F₅ and is the same trend for (HL⁺)Pt^{II}R₂, becoming more dominant over the platinum(IV) isomer LPt^{IV}R₂H⁺. There are several literature examples of *anionic* pentafluorophenylplatinum(II) complexes [Pt(C₆F₅)₃L''][–], with L'' containing a potential hydrogen bond donor group HX located in proximity to the metal atom.^{9,17} In the case of structurally similar substituted pyridine ligands with weakly acidic HX donors, such as H–C(sp³), H–C(sp²), and H–O–C(sp³), no H–Pt coupling was observed, and thus, no hydrogen bonding by this criterion was found in solution.¹⁷ In contrast, L'' with the more acidic phenolic hydroxyl, H–O–C(sp²), showed the presence of such an interaction.⁹ Since the pyridinium fragment NH⁺ is more acidic than the phenolic OH, we can rationalize why the uncharged and less electron-rich platinum(II) center in (HL⁺)Pt^{II}(C₆F₅)₂ exhibits Pt^{II}⋯H hydrogen bonding. Some degree of flexibility of the macrocycle L allows certain variation of the Pt–HN⁺ separation. The platinum(II) center in the case of R = Me is so electron-rich that the platinum(II) isomer, eq 3, is no longer thermodynamically preferred and can be observed only under conditions of kinetic control.

Thus, the basicities of a platinum(II) center toward two different acids, external H⁺ (as reflected by the position of equilibrium 3) and NH⁺ (as reflected by the value of the ¹J_{Pt–H} coupling constant in (HL⁺)PtR₂ species), correlate one with the other.

Conclusions

While this paper began by describing two *distinct* mechanistic possibilities for C–H cleavage, eqs 1 and 2, the fact that our compounds show equilibrium *interconversion* between the distinct products of these two mechanisms means that we are unable to make a mechanistic determination in our examples, from the available observations of CH bond cleavage. However, the evidence that these products, Pt^{II} and Pt^{IV}, are in hydrocarbyl-ligand-dependent equilibrium is an exceptional case of intramolecular migration between two redox states via bond breaking and making to H. Such redox isomerization is certainly facilitated by the hydrogen bonding, which in turn is another benefit of the "preorganized" geometry of the pyridinophane ligand on Pt^{II}.¹

Experimental Section

General Procedures. All manipulations were carried out under purified argon using standard Schlenk and glovebox techniques. Solvents were dried and distilled following standard protocols and stored in gastight bulbs under argon. All reagents for which a synthesis is not given are commercially available from Aldrich or Pressure Chemicals and were used as received without further purification. All NMR solvents were dried, vacuum-transferred, and stored in an argon-filled glovebox. [2.1.1]-(2,6)-Pyridinophane¹ and LPtMe₂¹⁴ have been synthesized according to the published procedures. ¹H and ¹⁹F NMR spectra were recorded on an Inova 700 spectrometer (¹H, 400 MHz; ¹⁹F, 376.43 MHz). ¹H and ¹⁹F NMR chemical shifts are reported in parts per million and referenced to residual solvent resonance peaks in the first two cases or the BAR^F₄ peak.

Synthesis of [(HL⁺)Pt^{II}(C₆F₅)₂]BAR^F₄. A 2 mL Schlenk flask equipped with a Kontes Teflon valve and magnetic stirring bar was charged in an argon-filled glovebox with 20 mg of NaBAR^F₄ (22 μmol), 20 μmol of LPtMe₂, and 0.6 mL of a 3:1 CD₂Cl₂–pentafluorobenzene mixture. The flask was then removed from the glovebox and immersed into an acetone bath cooled to –95 °C. The Teflon valve was replaced with a serum cap, and a solution of 3.0 mg of HSO₃CF₃ in 0.1 mL of CD₂Cl₂ (20 μmol) was added to the stirred suspension dropwise with a syringe. After 5 min of stirring at –95 °C the resulting liquid was warmed to room temperature and transferred to a Teflon-sealed NMR tube. Reaction was monitored by ¹H NMR spectroscopy. In 1 day at 22 °C the reaction was complete. Heating the reaction mixture at 80 °C in a sealed NMR tube for 96 h did not change its composition. Colorless crystals suitable for X-ray analysis were obtained by adding cyclohexane and allowing the mixture to evaporate slowly. Yield: 90%.

[(HL)Pt(C₆F₅)₂]BAR^F₄, Data for the Cationic Part. ¹H NMR (CD₂Cl₂, 22 °C): δ 3.31 (m, 1H, C₂H₄), 3.50 (ddd, *J* = 3.1, 13.5, 19.8 Hz, 1H, C₂H₄), 4.11 (m, 1H, C₂H₄), 4.22 (d, ²J_{H–H} = 14.1 Hz, 1H, CH₂), 4.54 (d, ²J_{H–H} = 15.3 Hz, 1H, CH₂), 4.81 (ddd, *J* = 2.9, 13.6, 15.9 Hz, 1H, C₂H₄), 5.46 (d, ²J_{H–H} = 14.0 Hz, 1H, CH₂), 6.17 (d, ²J_{H–H} = 15.2 Hz, 1H, CH₂), 7.42 (d, ³J_{H–H} = 7.8 Hz, 1H, *m*-CH, py), 7.54 (d, ³J_{H–H} = 7.8 Hz, 1H, *m*-CH, py), 7.59 (d, ³J_{H–H} = 8.0 Hz, 1H, *m*-CH, py), 7.65 (d, ³J_{H–H} = 7.8 Hz, 1H, *m*-CH, py), 7.66 (d, ³J_{H–H} = 7.9 Hz, 1H, *m*-CH, py), 7.83 (t, ³J_{H–H} = 7.9 Hz, 1H, *p*-CH, py), 7.86 (t, ³J_{H–H} = 7.8 Hz, 1H, *p*-CH, py), 8.19 (t, ³J_{H–H} = 8.0 Hz, 1H, *p*-CH, py), 16.33 (br s, 1H, NH). The NH⁺ proton signal is very broad at 22 °C (half-width of 57 Hz), thus making locating platinum satellites unreliable. The narrower signal of the NH⁺ proton observed at –40 °C (half-width of 21 Hz) resolved the value of ¹J_{Pt–H} = 63 Hz. ¹⁹F NMR (CD₂Cl₂, –40 °C): δ –164.40 (ddd, *J* = 8.1, 20.3, 29.7 Hz, 1F, *m*-CF), –164.09 (ddd, *J* = 8.3, 20.6, 29.7 Hz, 1F, *m*-CF), –163.14 (ddd, *J* = 8.3, 20.8, 29.2 Hz, 1F, *m*-CF), –162.90 (ddd, *J* = 8.1, 20.5, 29.2 Hz, 1F, *m*-CF), –161.05 (t, ³J_{F–F} = 20.3 Hz, 1F, *p*-CF), –160.93 (t, ³J_{F–F} = 20.3 Hz, 1F, *p*-CF), –122.12 (d, ³J_{F–F} = 29.2 Hz, ³J_{Pt–F} = 443 Hz, 1F, *o*-CF), –121.78 (d, ³J_{F–F} = 29.2 Hz, ³J_{Pt–F} = 446 Hz, 1F, *o*-CF), –119.31 (m, ³J_{Pt–F} = 408 Hz, 1F, *o*-CF), –118.68 (m, ³J_{Pt–F} = 416 Hz, 1F, *o*-CF). ¹⁹F NMR (CD₂Cl₂, 22 °C): δ –164.17 (br m, 2F, *m*-CF), –163.22 (br m, 2F, *m*-CF), –160.96 (t, ³J_{F–F} = 20.0 Hz, 1F, *p*-CF), –160.79 (t, ³J_{F–F} = 20.0 Hz, 1F, *p*-CF), –122.11 (br s, ³J_{Pt–F} = 440 Hz, 2F, *o*-CF), –119.01 (br m, ³J_{Pt–F} = 400 Hz, 2F, *o*-CF).

Attempted Reaction of [(HL⁺)Pt^{II}(C₆F₅)₂]BAR^F₄ with Cyclopentane. In an argon-filled glovebox a Teflon-capped NMR tube was charged with 16.8 mg of (HL⁺)Pt(C₆F₅)₂BAR^F₄ (10 μmol) and

(17) Casas, J. M.; Fornies, J.; Martin, A. *J. Chem. Soc., Dalton Trans.* **1997**, 1559.

0.6 mL of a 3:1 CD₂Cl₂–cyclopentane mixture. The tube was then removed from the glovebox and immersed into an oil bath preheated to 80 °C. After 24 h of heating the reaction mixture showed no changes in the ¹H NMR spectrum. In particular, no high-field Pt–H resonance due to LPtH(cyclopentane)⁺² was observed.

Protonation of LPt^{II}Me₂ and Thermal Transformation of [(HL⁺)Pt^{II}Me₂]BAR^F₄. A 2 mL Schlenk flask equipped with a Kontes Teflon valve, sealed NMR tube, and magnetic stirring bar was charged in an argon-filled glovebox with 20 mg of NaBAR^F₄ (22 μmol), 20 μmol of LPtMe₂, and 0.6 mL of CD₂Cl₂. The flask was then removed from the glovebox and immersed into an acetone bath cooled to –95 °C. The Teflon valve was replaced with a serum cap, and a solution of 3.0 mg of HSO₃CF₃ in 0.1 mL of CD₂Cl₂ (20 μmol) was added to the stirred suspension dropwise with a syringe. After 5 min of stirring at –95 °C the resulting liquid was transferred into a sealed NMR tube precooled with the acetone bath. The flask was connected to a vacuum line, and the NMR tube was flame-sealed. Reaction was monitored by ¹H NMR spectroscopy in a precooled NMR probe starting from –80 °C. The temperature was raised by 10° increments. At –80 °C three isomeric products were observed, (HL⁺)Pt^{II}Me₂ (8%), unsym-LPt^{IV}Me₂H⁺ (88%), and sym-LPt^{IV}Me₂H⁺ (4%).³ They underwent quantitative isomerization into sym-LPt^{IV}Me₂H⁺ in the temperature range of –50 to –30 °C. To follow the (HL⁺)Pt^{II}Me₂ to sym-LPt^{IV}Me₂H⁺ isomerization, spectra were taken every 10 min at a constant temperature, –45 °C. The approximate half-life for (HL⁺)Pt^{II}Me₂ undergoing isomerization into sym-LPt^{IV}Me₂H⁺ at the temperature given was calculated to be 8 min.

[(HL)Pt^{II}Me₂]BAR^F₄, Data for the Cationic Part. ¹H NMR (CD₂Cl₂, –65 °C): δ: 0.64 (s, ²J_{Pt–H} = 84 Hz, 3H, PtMe), 0.69 (s, ²J_{Pt–H} = 86 Hz, 3H, PtMe), 4.03 (d, ²J_{H–H} = 15.4 Hz, 1H, CH₂), 4.21 (d, ²J_{H–H} = 14.0 Hz, 1H, CH₂), 4.88 (d, ²J_{H–H} = 15.4 Hz, 1H, CH₂), 5.26 (d, ²J_{H–H} = 14.0 Hz, 1H, CH₂), 7.21 (d, ³J_{H–H} = 7.8 Hz, 1H, *m*-CH, py), 7.36 (d, ³J_{H–H} = 7.8 Hz, 1H, *m*-CH, py), 7.40 (d, ³J_{H–H} = 7.8 Hz, 1H, *m*-CH, py), 7.44 (d, ³J_{H–H} = 7.8 Hz, 1H, *m*-CH, py), 7.95 (t, ³J_{H–H} = 7.8 Hz, 1H, *p*-CH, py), 17.17 (br s, ¹J_{Pt–H} = 90 Hz, 1H, Pt···HN); signals of two *m*-CH and two *p*-CH groups presumably overlap with the other signals.

[unsym-LPt^{IV}Me₂H]BAR^F₄, Data for the Cationic Part. ¹H NMR (CD₂Cl₂, –65 °C): δ: –22.23 (s, ¹J_{Pt–H} = 1373 Hz, 1H, PtH), 1.17 (s, ²J_{Pt–H} = 69 Hz, 3H, PtMe), 1.45 (s, ²J_{Pt–H} = 69 Hz, 3H, PtMe), 3.08 (m, 1H, C₂H₄), 3.09 (m, 1H, C₂H₄), 3.47 (m, 1H, C₂H₄), 4.09 (d, ²J_{H–H} = 15.1 Hz, 1H, CH₂), 4.32 (d, ²J_{H–H} = 15.0 Hz, 1H, CH₂), 4.53 (m, 1H, C₂H₄), 4.71 (d, ²J_{H–H} = 15.0 Hz, 1H, CH₂), 4.82 (d, ²J_{H–H} = 15.0 Hz, 1H, CH₂), 7.13 (d, ³J_{H–H} = 8.0 Hz, 1H, *m*-CH, py), 7.27 (d, ³J_{H–H} = 8.0 Hz, 1H, *m*-CH, py), 7.30 (d, ³J_{H–H} = 8.0 Hz, 1H, *m*-CH, py), 7.32 (d, ³J_{H–H} = 8.0 Hz, 1H, *m*-CH, py), 7.48 (d, ³J_{H–H} = 8.0 Hz, 1H, *m*-CH, py), 7.49 (d, ³J_{H–H} = 8.0 Hz, 1H, *m*-CH, py), 7.54 (t, ³J_{H–H} = 7.8 Hz, 1H, *p*-CH, py), 7.64 (t, ³J_{H–H} = 7.8 Hz, 1H, *p*-CH, py), 7.77 (t, ³J_{H–H} = 7.8 Hz, 1H, *p*-CH, py).

X-ray Structure Determination of [(LH⁺)Pt(C₆F₅)₂](BAR^F₄). A colorless crystal (approximate dimensions 0.20 × 0.15 × 0.13

mm³) was placed onto the tip of a 0.1 mm diameter glass capillary and mounted on a SMART6000 (Bruker) at 137(2) K.

The data collection was carried out using Mo Kα radiation (graphite monochromator) with a frame time of 10 s and a detector distance of 5.1 cm. A randomly oriented region of two spheres in reciprocal space was surveyed. Six major sections of frames were collected with 0.30° steps in ω at six different φ settings and a detector position of –43° in 2θ. An additional set of 50 frames was collected to model decay. Data to a resolution of 0.71 Å were considered in the reduction. Final cell constants were calculated from the xyz centroids of 9604 strong reflections from the actual data collection after integration (SAINT).¹⁸ The intensity data were corrected for absorptions (SADABS).¹⁹ Table 1 contains additional crystal and refinement information.

Structure Solution and Refinement. The space group *P*2₁/*c* was determined on the basis of intensity statistics and systematic absences. The structure was solved using SIR-92²⁰ and refined with SHELXL-97.²¹ A direct-methods solution was calculated which provided most non-hydrogen atoms from the *E*-map. Full-matrix least-squares/difference Fourier cycles were performed which located the remaining non-hydrogen atoms. All non-hydrogen atoms were refined with anisotropic displacement parameters. The hydrogen atoms were placed in ideal positions and refined as riding atoms with relative isotropic displacement parameters with the exception of H1n, which was refined with an individual displacement parameter. The structure contains large voids (1576 Å³ per unit cell) that are occupied by dichloromethane molecules. Their contribution to the structure factors was assessed by back Fourier transformation to 132 electrons per unit cell; for comparison, dichloromethane occupies 83 Å³ with 78 electrons.²² The data were modified accordingly. The refinement using the modified dataset improved the overall structure and the *R* values significantly. The remaining electron density is located in the vicinity of the CF₃ groups. One CF₃ group is disordered over two positions.

Acknowledgment. This work was supported by the DOE. A.N.V. is on leave from the Chemical Faculty, Kazan State University, Kazan, Russia. This work has been made possible in part due to support from the Russian Foundation for Basic Research (Grant 01.03.32692).

Supporting Information Available: Full crystallographic details (CIF, PDF). This material is available free of charge via the Internet at <http://pubs.acs.org>.

IC034731M

(18) SAINT 6.1, Bruker Analytical X-ray Systems, Madison, WI.

(19) Blessing, R. *Acta Crystallogr.* **1995**, *A51*, 33.

(20) Altomare, A.; Cascarno, G.; Giacovazzo, C.; Gualardi, A. *J. Appl. Crystallogr.* **1993**, *26*, 343.

(21) SHELXTL-Plus V5.10, Bruker Analytical X-ray Systems, Madison, WI.

(22) Immirzi, A.; Perini, B. *Acta Crystallogr.* **1977**, *A33*, 216.